

Deterministic Method to Assess Kalman Filter Passive Ranging Solution Reliability

Ronald M. Yannone

Abstract—For decades, the defense business has been plagued by not having a reliable, deterministic method to know when the Kalman filter solution for passive ranging application is reliable for use by the fighter pilot. This has made it hard to accurately assess when the ranging solution can be used for situation awareness and weapons use. To date, we have used ad hoc rules-of-thumb to assess when we think the estimate of the Kalman filter standard deviation on range is reliable. A reliable algorithm has been developed at BAE Systems Electronics & Integrated Solutions that monitors the Kalman gain matrix elements – and a patent is pending. The “settling” of the gain matrix elements relates directly to when we can assess the time when the passive ranging solution is within the 10 percent-of-truth value. The focus of the paper is on surface-based passive ranging – but the method is applicable to airborne targets as well.

Keywords—Electronic warfare, extended Kalman filter (EKF), fighter aircraft, passive ranging, track convergence.

I. INTRODUCTION

THE use of passive sensor angle measurements to compute the location of surface and airborne radio frequency (RF) emitters (also called targets in this paper) for low observable fighter aircraft is vital to ensure mission success and pilot survivability [1]. The onboard electronic warfare (EW) sensor suite consists of multiple short baseline interferometers (SBI) that detect the radar emissions from the emitters in the battle space. The angle measurement accuracy is a function of emitter frequency, emitter angle-off-array-boresight, SBI array length, the signal-to-noise ratio, the number of RF pulses processed by the EW system, and overall array phase error. The SBI parameters consequently yield different 1-sigma values over time. Because the EW system has no control over the emitters, the measurements come arrive either synchronously or asynchronously. The sensor may also be on unmanned aerial vehicles (UAV).

The fighter aircraft flies straight-and-level with pre-planned, coordinated heading changes at way points in the mission. In the course of a mission, the pilot will encounter unexpected pop-up surface or airborne emitters that he needs to either avoid or respond to quickly. Pilot responses may include the use of defensive or offensive weapons – or a simple change in aircraft orientation with respect to the emitter (weapon system). In both cases, the EW system processes SBI measurements. Sometimes the EW system will be able to regulate the measurement update rate – and this can assist convergence in the passive ranging solution.

The methodology to analyze extended Kalman filter (EKF) tracking performance is to define a scenario. A scenario is defined using the initial range and azimuth angle to the surface emitter, as well as the fighter platform speed and heading, total scenario time, and measurement update rate. The analysis can be extended to the slow-moving surface emitter, as well as the airborne emitter. The past effort used fixed-gain alpha-beta filters – with stored gains. The use of the 1-sigma value from the Kalman filter was used next for years – where a fudge factor is multiplied by the 1-sigma value (like 3 or 3.5) and this has always been like the throw of the dice in actuality. This ad hoc approach was used for over a decade and proven unreliable for the end-user. The next section summarizes previous related work we examined.

II. REVIEW OF PREVIOUSLY RELATED WORK

The author's personal experience in developing passive, angle-only target tracking began at General Electric Company's Aerospace & Electronic Systems Department (AESD) in Utica, New York in the late 1970s using the infrared search and track (IRST) sensor intensity and angle data on F-15 aircraft; electronic warfare sensors that provide RF parameters and angle data; and cooperative aircraft angle-based tracking. Stealthy operation was a principal driver. The Kalman filter was the basic algorithm building block – which we discuss in more detail in this paper. Thousands of papers on Kalman filtering exist. The first available books used were by Arthur Gelb (copyright 1974) on Kalman filtering and Harry Van Trees (1968) on the Cramer-Rao lower bound (CRB) [2, 3]. Principal former technical papers we explored are given in references [4-6]. These papers review “observability” from an estimation view (vs. fighter aircraft stealth radar-cross-section “observability”) and the CRB. The CRB is the theoretical estimation performance for the scenario, independent of the implementation used by the designer to process the noisy measurements. The procedure involves writing the equations for the N measurements as functions of the M state variables to be estimated. The partial derivatives of each measurement equation are computed w.r.t. the M state variables to be estimated. These partial derivatives of the measured parameters with respect to the state variables are placed into the H matrix with N rows and M columns. If the measurement errors are jointly Gaussian and if the estimation error distribution can be approximated by a joint Gaussian function, then the CRB can be determined by $C =$

$(H^T R^{-1} H)^{-1}$. In this expression, R is the N -by- N covariance matrix for the measurement errors. The standard deviation of the M th parameter to be estimated is the square root of the (M, M) entry in C . The inverse of the matrix C is referred to as the Fisher Information Matrix. If the measurement errors are uncorrelated, jointly Gaussian, and have the same variance, then $C = R(H^T H)^{-1}$. A simulation involves constructing the H matrix over the cumulative number of measurements for the scenario using the true state variables and the measurement error covariance matrix, R , to compute C , and then using the square root of the appropriate diagonal element to determine its standard deviation. All simulation and modeling of algorithms included the CRB and the algorithm-under-test 1-sigma range estimates for passive ranging. The CRB is a benchmark to see if the algorithm has the ability to reach theoretical estimation performance. Real systems are the proof-of-the pudding; and often the 1-sigma range value provided by different algorithms was rarely “representative” of the true value. This has remained a big concern for our customers – especially current customers – until recent research in 2005 that explored the Kalman filter gain elements.

III. SAMPLE TRACKING SCENARIO REVIEW STAGE

The six inputs to a Monte Carlo MATLAB m-file are:

- D(1) - initial slant range in nautical miles (R_{slant})
- D(2) - initial azimuth angle in degrees (AZ)
- D(3) - ownship height in kilo-feet (H)
- D(4) - ownship speed in knots (V)
- D(5) - scenario duration in seconds (t)
- D(6) - sample interval in seconds (d_t)

The user completes the line below with the six parameters in brackets [R_{slant} , AZ , H , V , t , d_t] to create a data vector.

Parameters within the m-file the user selects include: angle measurement accuracy for the elevation and azimuth cone angle; the seeded initial range and the corresponding sigma range. The user can experiment with other EKF internal matrix components, like the process noise error covariance matrix (Q), initial state vector error covariance matrix (P_{init}), and initial state vector (X_{init}). The m-file provides the following plots listed in Table 1. The four plots are presented below. In this example, the SBI azimuth 1-sigma value is 1 degree and 1-sigma elevation is 1 degree.

TABLE I
PLOTS THE DESIGNER ANALYZES

PLOT	PARAMETER(S)
1	horizontal range, slant range, spherical azimuth, spherical elevation
2	spherical and SBI cone angle; cone angle rate, spherical AZ and elevation (EL) angle rate
3	true and estimate cone angle from the EKF
3	measurement residual in the cone angle (estimated minus true cone angle)
3	single Monte Carlo plot of true and estimated range from the EKF
4	Monte Carlo results of true and EKF-based percent range error (PRE) — overlaid with the Cramer-Rao lower bound

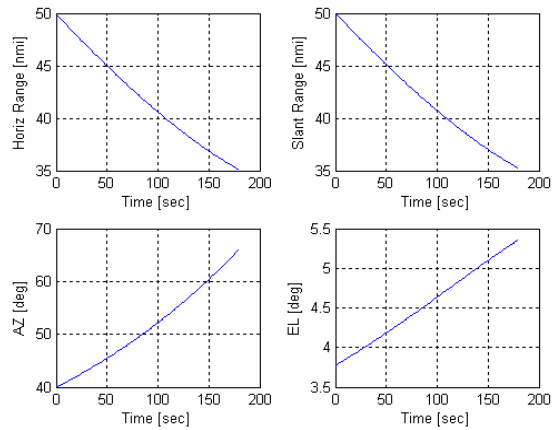


Fig. 1 Scenario horizontal range, slant range, spherical AZ and EL

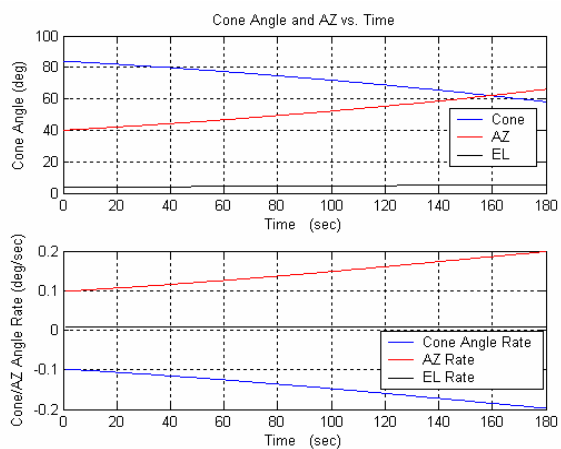


Fig. 2 Spherical and SBI cone angle; cone angle rate, spherical AZ and EL angle rate

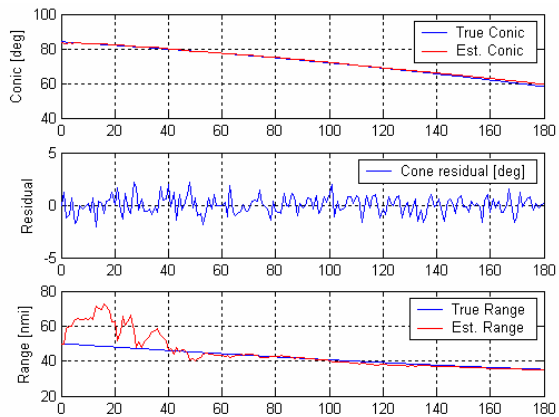


Fig. 3 True/estimated cone angle, cone angle residual, single Monte Carlo true/estimated range

Examining the figures produced by the m-file, the designer can get a feel for the EKF performance. The standard deviation of range, expressed as a percentage of the final value of the final range, is given by 100 times the square root of the (M, M) entry corresponding to the range parameter in C , divided by the final range. The designer would like tracker

performance to be close to the CRB value. Based on 3rd and 4th plots, the designer historically developed ad hoc rule-based algorithms to quantify when they felt the EKF could be confident in its 1-sigma range estimate. This usually was very scenario dependent and many times like the roll-of-dice!

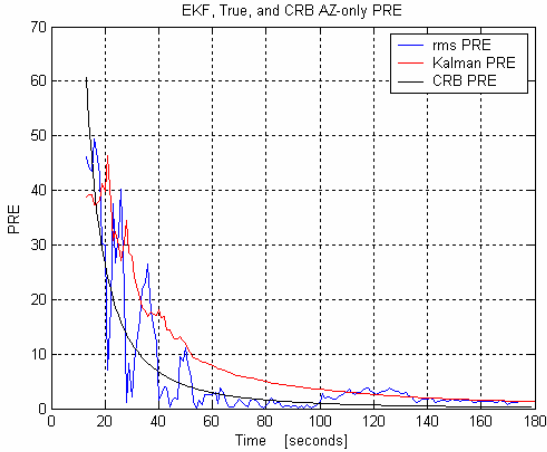


Fig. 4 Monte Carlo RMS True PRE and EKF Estimated PRE

The dilemma the designer faced in the past was looking at plots of percent range error (PRE) – Figure 4 – where he/she tries to conjure up a rule for declaring when they felt the EKF was producing a reliable result. The Cramer-Rao lower bound is the theoretical bound on passive ranging performance independent of the algorithm mechanization used. This has been an endless effort. Next we look at the five basic Kalman filter equations and focus on the EKF matrix that provides the probe we need.

IV. KALMAN FILTER DESCRIPTION

The Kalman filter equations are as follows [2]

$$\tilde{\hat{X}} = \Phi \hat{X} + \text{Ownship} \quad (1)$$

$$\tilde{P} = \Phi \hat{P} \Phi^T + Q \quad (2)$$

$$K = \tilde{P} H^T (H \tilde{P} H^T + R)^{-1} \quad (3)$$

$$\hat{P} = (I - KH) \tilde{P} (I - KH)^T + K R K^T \quad (4)$$

$$\hat{X} = \tilde{\hat{X}} + K(z - f(\tilde{\hat{X}})) \quad (5)$$

The Kalman filter is a recursive computational algorithm that processes measurements (z) to deduce a minimum variance, unbiased error estimate of the state (\hat{X}) of a system by utilizing knowledge of system (i.e., the state equation, and state transition matrix (Φ) and measurement (functional – $f(\tilde{\hat{X}})$) dynamics, assumed statistics of the system noises (Q -matrix) and measurement errors (R -matrix), and initial condition information (\hat{X} and \hat{P}). The Ownship vector accounts for the fighter aircraft motion over the measurement interval; I is the identity matrix; K is the Kalman gain matrix; and $(z - f(\tilde{\hat{X}}))$ is the residual.

The Ownship vector accounts for the fighter aircraft motion over the measurement interval; I is the identity matrix; K is the Kalman gain matrix; and $(z - f(\tilde{\hat{X}}))$ is the residual. The expression for \hat{P} is the Joseph form for the error covariance update.

The Kalman filter stability (robustness) can be understood by the Table II. This becomes very important when we process combined AZ/EL measurements for estimating parameters for constant speed, constant heading airborne targets passively using passive ranging fighter maneuvers. Under this mode of operation we use a patent-pending algorithm that exploits the interacting multiple model (IMM). See U.S. Patents and Trademarks website (patent filing # 20050110661). In the IMM, the residuals automatically adapt the tracker to handle non-maneuvering and maneuvering airborne targets.

TABLE II
KALMAN FILTER STABILITY/ROBUSTNESS RELATIONSHIPS

EIGENVALUES (DISCRETE TIME) – [Z-PLANE]	COMMENT	POLE LOCATIONS (CONTINUOUS-TIME) – [S-PLANE]
$\lambda(\Phi - KH) < 1$	stable	left-half plane poles
$\lambda(\Phi - KH) = 1$	marginally stable	j ω -axis poles
$\lambda(\Phi - KH) > 1$	unstable	right-half plane poles

- K is a function of the time-extrapolated error covariance matrix – \tilde{P}
- P_{tilde} is a function of the process noise error covariance matrix – Q
- Filter transient response varies with the system pole locations
- The deterministic input to the Kalman filter which gives an indication that the target is maneuvering (i.e., deviating from a prescribed flight path) are the measurement residuals
- Therefore the measurement residuals can be used to regulate Q , and Q regulates the Kalman filter bandwidth/robustness/stability

For passive ranging against surface emitters, we have excellent knowledge of the target dynamics model – namely it is a constant speed, constant heading target with zero speed and zero heading – so the 3-by-3 process noise covariance matrix (Q) is “zero” and the state transition matrix (Φ) is the 3-by-3 identity matrix. Not given in this paper are the specific initial state vector and companion initial error covariance matrix – and this does not detract from the algorithm being addressed in this paper – namely the deterministic assessment of when the EKF range estimate is reliable.

The number of state variables is n and measurements m , so we have dimensions for the various Kalman filter parameters as summarized in Table III. We use $n=3$ states $[x, y, z]$ to address slow-moving and stationary targets and $n=6$ states $[x, \dot{x}, y, \dot{y}, z, \dot{z}]$ to address airborne targets.

TABLE III
EKF MATRIX DIMENSIONS

PARAMETER	DIMENSION	PARAMETER	DIMENSION
state vectors (X)	n-by-1	state transition matrix	n-by-n
Ownship vector	n-by-1	functional	m-by-1
H matrices	m-by-n	P matrices	n-by-n
Q matrix	n-by-n	S matrix	m-by-m
R matrix	m-by-m	gain (K) matrix	n-by-m
z (measurement vector)	m-by-1	I matrix	n-by-n
residual	m-by-1	range estimate sigma	1-by-1

We process either single azimuthal SBI conic measurements or both azimuthal and elevation SBI conic measurements – depending on the specific EW system sensor asset selected. The north-west-up wander angle system is used to process the measurements and the results are transformed into spherical AZ or AZ/EL and slant range for the onboard Mission Systems function. Mission Systems performs sensor fusion of all onboard sensor data, as well as offboard information from wingmen (friendly nearby aircraft), long-range surveillance assets, and national overhead assets. The designer controls different internal EKF parameters, as summarized in Table IV.

TABLE IV
USER HAS PARAMETERS TO “ADJUST” IN THE KALMAN FILTER DESIGN PROCESS

PARAMETER	COMMENTS
Initial State Vector – X	The initial state 3-by-1 state vector can be “filled in” based on the initial range guess and the first azimuth measurement. This uses $x = R_guess * \cos(AZ_0)$, $y = R_guess * \sin(AZ_0)$. When EL measurements are made, we can define $z = -R * \sin(EL_0)$ or simply the altitude difference between the sensor and earth’s surface
Initial State Vector Error Covariance matrix - P	The initial state vector error covariance matrix (P_hat) uses the initial range and angle measurements and their accuracy values (i.e., the R matrix values); the 1-sigma range estimate value; as well as the 1-sigma range rate estimate; being able to bound these aids filter convergence to the true state variables; for the airborne application it is possible to bound the target speed region
Process Noise Error Covariance Matrix - Q	Process noise covariance matrix (Q) accounts for the uncertainty in the assumed target dynamics model (i.e., the state equation that defines the kinematic physics of the problem) with $Q = 0$, we say we know the assumed target dynamics model is correct – while a large-value Q matrix indicates that we are uncertain in the assumed target dynamics model and thus directs the Kalman filter to “weight” (use) the measurements heavily

By analyzing the different EKF matrices, it turns out that the Kalman gain matrix elements provide the deterministic assessment as to when the EKF passive ranging solution is accurate to within 10 percent of the true range. Keep in mind we never know the true range so we need this reliable metric for the pilot to base his/her actions upon. In the next section we look at a spread of scenario geometries to give a feel for

how to characterize the EKF gain matrix-based assessment.

V. CHARACTERIZATION OF THE EKF GAIN-BASED ALGORITHM

Historically, to assess track convergence, we relied on a fudge factor multiplier of the Kalman filter’s estimate of the scalar quantity $\sigma_{range} = \sqrt{HPH^T}$, where H is the partial derivatives of range with respect to the three position state variables (x, y, z) and P is the measurement updated 3-by-3 symmetric error covariance matrix. To date the fudge factor has never been reliable much of the time. For the same scenario described in Section II, we plot the EKF gain matrix elements below in Fig. 5. Through extensive research at BAE Systems, we determined that the Kalman filter “settling characteristics” can be captured in its gain matrix elements. By monitoring these gain elements for the whole span of tracking engagements, we exhaustively parameterized their behavior. Namely, we varied the initial azimuth from [20, 80 degrees] and initial range between [20, 100 nautical miles]. This was performed with measurement update intervals between [0.5, 10 seconds]. No earlier publications were used in unveiling this – it was from an intuitive hunch from two decades of practical experience.

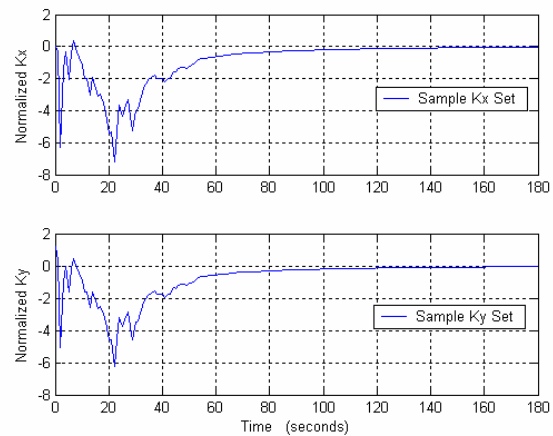


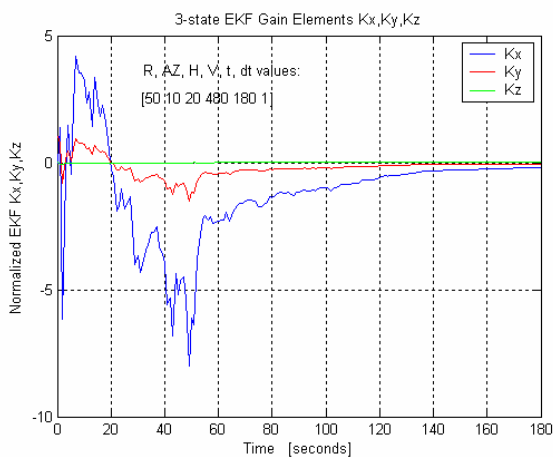
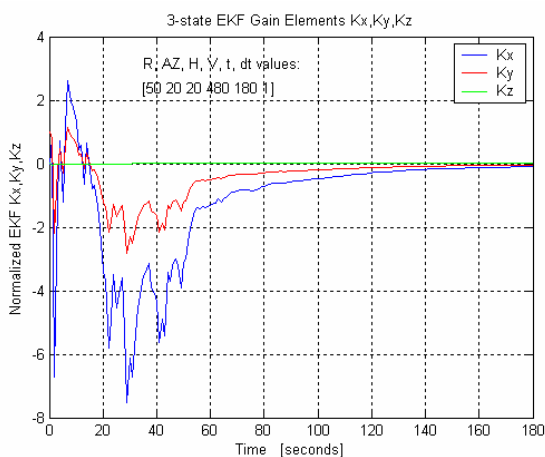
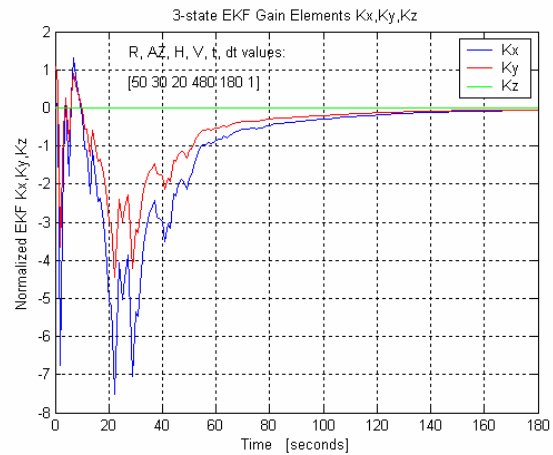
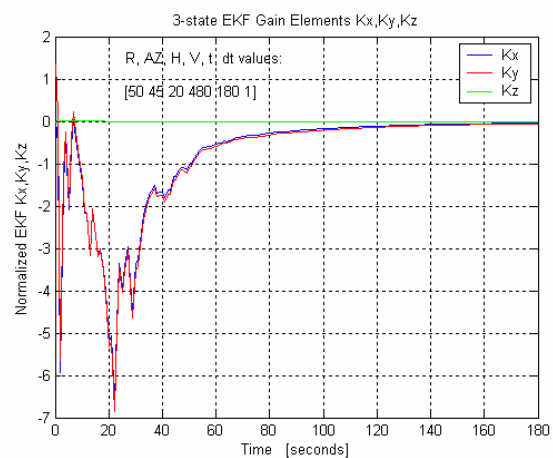
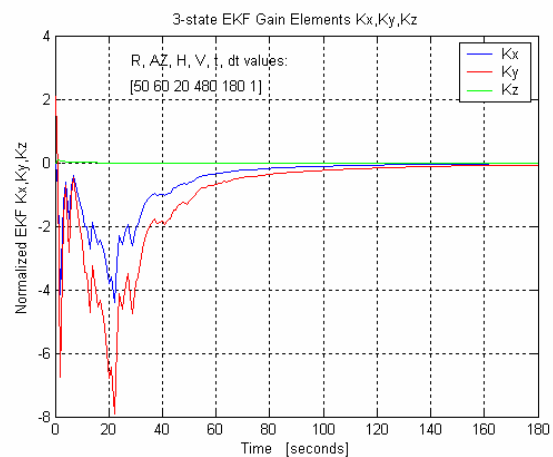
Fig. 5 The EKF Gain Matrix Element Values

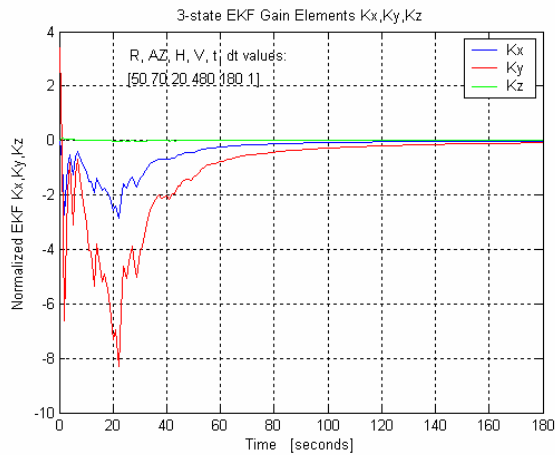
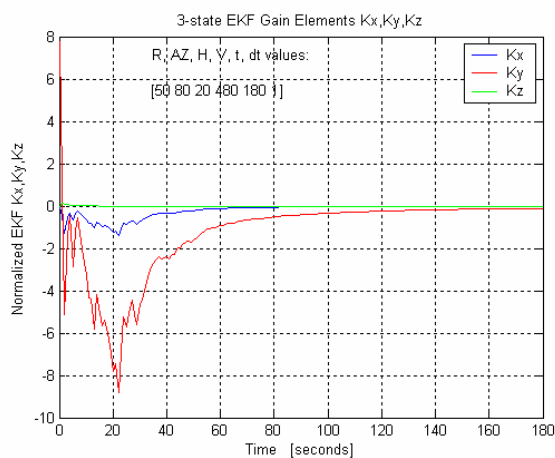
We make a few observations from Fig. 5. We then look at scenarios over initial AZ values between 10 to 80 degrees.

1. the x-component and y-component of the gain “follow” each other very closely in shape and closely in value. This occurs identically when the initial AZ for the scenario is 45 degrees
2. the EKF gain matrix element “settling” occurs at around 60 seconds – and this corresponds to when the true and EKF estimated percent range error (PRE) are within 10 percent of each other.
3. when the EKF gain matrix elements hit their minimum, the EKF “observability” kicks in – namely the filter has reached the point where a solution is definitely being converged on

Figs. 6 through 12 replicate the above scenario we exercised with the initial azimuth value, $AZ = 10, 20, 30, 45, 60, 70$, and 80 degrees. We make further observations:

4. the EKF z-component of the gain matrix plays a minimal part for very small fighter (sensor) altitude-to-slant-range ratios (i.e., long-range emitters). For all the scenarios of immediate interest to the fighter aircraft applications we are interested in the target is greater than or equal to 20 nautical miles
5. when the target initial AZ is close to the fighter nose, the x-component of the gain matrix is required to pull in the slant range estimate to a usable (low) error. The estimation system is said to be Kx-dominant
6. as the target initial AZ is close to the fighter right wing, the stronger the y-component of the gain matrix is required to pull in the slant range estimate to a usable (low) error. The estimation system is said to be Ky-dominant. This scenario is also defined as the case where the emitter is near the point-of-closest-approach (PCA)
7. the more accurate the angle measurement, the faster the minimum occurs for the appropriate Kx or Ky element – or both when the initial AZ in near the 45 degree region
8. passive ranging solution convergence is accelerated near the PCA, as the traversed-bearing-spread (TBS) per unit time is greater than the near-nose target geometry

Fig. 6 $[R, AZ, H, V, t, dt] = [50 \ 10 \ 20 \ 480 \ 180 \ 1]$ Fig. 7 $[R, AZ, H, V, t, dt] = [50 \ 20 \ 20 \ 480 \ 180 \ 1]$ Fig. 8 $[R, AZ, H, V, t, dt] = [50 \ 30 \ 20 \ 480 \ 180 \ 1]$ Fig. 9 $[R, AZ, H, V, t, dt] = [50 \ 45 \ 20 \ 480 \ 180 \ 1]$ Fig. 10 $[R, AZ, H, V, t, dt] = [50 \ 60 \ 20 \ 480 \ 180 \ 1]$

Fig. 11 $[R, AZ, H, V, t, dt] = [50 \ 70 \ 20 \ 480 \ 180 \ 1]$ Fig. 12 $[R, AZ, H, V, t, dt] = [50 \ 80 \ 20 \ 480 \ 180 \ 1]$

Algorithms are used to (1) analyze the EKF gain matrix K_x and K_y elements in real time via curve-fit routines to detect their absolute minimum values, and (2) assess the amount of “settling” of these elements to deterministically alert the pilot when the EKF passive ranging solution is within 10 percent of the true range. Typically a useful settling value is 1/16 for the desired 10 percent PRE indicator. This means the absolute value of the minimum dominant gain element (K_x , K_y , or K_z when the target AZ is close to 45 degrees) is multiplied by 1/16, and the time this result occurs is the desired cue time for the pilot.

BAE Systems is also developing algorithms that will back-fit the gain matrix element curve from the 10 percent time point to provide the pilot higher (less accurate) PRE values earlier that he/she can use for situation awareness and to book-mark emitters on the earth – for when it egresses and to forward the information to other assets (wingmen, Mission Systems, and national assets). What this means is if the 10 percent time is 60 seconds, the 20 through 50 percent time points can also be provided to the pilot earlier.

VI. CONCLUSION

We learned over the years, through several defense programs, that the sole use of the Kalman filter’s derived 1-sigma value for the range estimate is unreliable most of the time based on algorithms we’ve developed. Ad hoc rules never sufficed either. In some applications where the end-user needed a reliable indication that the filter’s estimate was “accurate,” they turned the system ‘off’ when it did not provide this indication reliably. No a priori research documented that we are aware of presented a solution. Our research showed that the deterministic method to accurately assess EKF track convergence for an azimuth-only system, prosecuting a fixed or slowly moving surface emitter target, is to monitor the gain matrix elements in real time. This entails curve-fitting the gain elements separately (K_x , K_y) over time, determining their individual minimum, and using a fraction of the ‘dominant’ gain element’s minimum (like 1/16 in our application) to search for the desired gain element “settling” time. The gain elements are equal for the case $AZ_0 = 45$ degrees – in which case either of the gain elements can be used. When the individual gain value reaches this attenuated value, then the range estimate will be within 10 percent of the true value. The method is very well prescribed – once the user has the complete set of sensor-target geometries to work against.

REFERENCES

- [1] N. Levanon, “Interferometry against Differential Doppler: Performance Comparison of Two Emitter Location Airborne Systems,” *IEEE Proceedings*, vol. 136, Pt. F., No 2, April 1989, pp. 70-74.
- [2] A. Gelb, “Applied Optimal Estimation,” 15th printing, The M.I.T. Press, 1999, pp. 102-155.
- [3] H. Van Trees, “Detection, Estimation, and Modulation Theory – Part I,” John Wiley & Sons, 1968, pp. 66-73.
- [4] S. Nardone, A. Lindgren, and K. Gong, “Fundamental Properties and Performance of Conventional Bearings-Only Target Motion Analysis,” *IEEE Transactions on Automatic Control*, vol. AC-29, no. 9, Sept. 1984, pp. 775-787.
- [5] M. Gavish and A. Weiss, “Performance Analysis of Bearing-Only Target Location Algorithms,” *IEEE Transactions on Aerospace and Electronic Systems*, vol. 28, no.3, July 1992.
- [6] S. Koteswara Rao, “Maximum Likelihood and Cramer-Rao Lower Bound for (Nonlinear) Bearing Only Passive Target Tracking,” *Conference Record of the Thirty-Second Asilomar Conference on Signals, Systems & Computers*, Nov. 1998, vol. 1, pp. 441-444.